HAL
open science

Charge Transport and Electrical Properties of Spin Crossover Materials: Towards Nanoelectronic and Spintronic Devices

Constantin Lefter, Vincent Davesne, Lionel Salmon, Gábor Molnár, Philippe Demont, Aurelian Rotaru, Azzedine Bousseksou

To cite this version:

Constantin Lefter, Vincent Davesne, Lionel Salmon, Gábor Molnár, Philippe Demont, et al.. Charge Transport and Electrical Properties of Spin Crossover Materials: Towards Nanoelectronic and Spintronic Devices. Magnetochemistry, 2016, 2 (1), pp.18. 10.3390/magnetochemistry2010018 . hal-01346000

HAL Id: hal-01346000

https://hal.science/hal-01346000v1

Submitted on 18 Jul 2016

HAL is a multi-disciplinary open access archive for the deposit and dissemination of scientific research documents, whether they are published or not. The documents may come from teaching and research institutions in France or abroad, or from public or private research centers.

L'archive ouverte pluridisciplinaire **HAL**, est destinée au dépôt et à la diffusion de documents scientifiques de niveau recherche, publiés ou non, émanant des établissements d'enseignement et de recherche français ou étrangers, des laboratoires publics ou privés.

Open Archive TOULOUSE Archive Ouverte (OATAO)
OATAO is an open access repository that collects the work of Toulouse researchers and makes it freely available over the web where possible.

This is an author-deposited version published in : http://oatao.univ-toulouse.fr/
Eprints ID : 15719

To link to this article : 10.3390/magnetochemistry2010018
URL : http://dx.doi.org/10.3390/magnetochemistry2010018

To cite this version : Lefter, Constantin and Davesne, Vincent and Salmon, Lionel and Molnar, Gabor and Demont, Philippe and Rotaru, Aurelian and Bousseksou, Azzedine *Charge Transport and Electrical Properties of Spin Crossover Materials: Towards Nanoelectronic and Spintronic Devices.* (2016) Magnetochemistry, vol. 2 (n° 1). pp. 1-19. ISSN 2312-7481

Any correspondence concerning this service should be sent to the repository administrator: staff-oatao@listes-diff.inp-toulouse.fr

Charge Transport and Electrical Properties of Spin Crossover Materials: Towards Nanoelectronic and Spintronic Devices

Constantin Lefter [1,2,†], Vincent Davesne [1,†], Lionel Salmon [1], Gábor Molnár [1], Philippe Demont [3], Aurelian Rotaru [2] and Azzedine Bousseksou [1,*]

[1] LCC, CNRS & Université de Toulouse (UPS, INP), 205 route de Narbonne, Toulouse 31077, France; colefter@eed.usv.ro (C.L.); vincent.davesne@lcc-toulouse.fr (V.D.); lionel.salmon@lcc-toulouse.fr (L.S.); gabor.molnar@lcc-toulouse.fr (G.M.)

[2] Faculty of Electrical Engineering and Computer, Stefan cel Mare University of Suceava, Str. Universitatii nr. 13, Suceava 720229, Romania; aurelian.rotaru@gmail.com

[3] Institut Carnot-CIRIMAT, Université de Toulouse, 118 route de Narbonne, Toulouse 31062, France; philippe.demont@univ-tlse3.fr

* Correspondence: azzedine.bousseksou@lcc-toulouse.fr; Tel.: +33-(0)5-6133-3169; Fax: +33-(0)5-6155-3003

† These authors contributed equally to this work.

Abstract: In this paper, we present a comprehensive review of research on electrical and charge transport properties of spin crossover complexes. This includes both the effect of spin-state switching on the dielectric permittivity and electrical conductivity of the material and *vice versa* the influence of an applied electrical field (or current) on the spin-state of the system. The survey covers different size scales from bulk materials and thin films to nanoparticles and single molecules and embraces the presentation of several device prototypes and hybrid materials as well.

Keywords: charge transport; dielectric permittivity; electronic device; spin crossover

1. Introduction

Switchable molecular materials have been in the research spotlight since the miniaturization of silicon based devices and conventional magnetic storage devices approaches the technological and physical limits [1–3]. In this context, the field of molecular electronics might bring some solutions with the use of molecular switches [4,5], single molecular magnets [6,7] or molecular logic gates [8–10]. Molecular switches can be switched between two different states (ON/OFF) characterized in some cases by different molecular structures (structural isomerization), electronic configurations or oxidation states (redox switches) [4]. Single molecular magnets exhibit slow relaxation of the magnetization at low temperatures and can exhibit striking quantum effects, like tunneling of the magnetization [11]. Molecular logic gates usually transform chemical, optical, electrical and magnetic inputs into different chemical, optical, electrical and magnetic outputs [9].

Among these molecular switches, spin crossover (SCO) compounds present a special interest due to the wide range of their potential applications. These transition metal complexes exhibit reversible switching between the so-called low spin (LS) and high spin (HS) electronic configurations [12–14]. The conversion between these two states can be triggered by various external stimuli such as temperature, pressure, light or X-ray irradiation, an intense magnetic field or the inclusion of guest molecules. The two spin states can then be distinguished by their different magnetic, optical, mechanical, spectroscopic and structural properties. The changes associated with the spin transition can propagate in a cooperative way [15], which can produce hysteresis phenomena even at room

temperature. An appealing aspect of the spin transition is that the switching of the electronic configuration can occur on a sub-ps time scale [16], which can translate into THz scale processing rate. From the technological point of view SCO materials have been proposed for numerous applications ranging from displays [17], memory devices [18], pressure and temperature sensors [19], gas sensors [20], nanothermometers [21], optoelectronic devices [22] and actuators [23].

Considering the vast applicability of these materials, several research groups have recently embarked on the study of electrical properties of SCO compounds including the possibility of their addressing by electrical field and/or current. The use of electrical stimuli to control (read/write) the spin-state of the system would provide a great advantage to other stimuli such as temperature or pressure due to a faster dynamics (less inertia), easier size reduction and better compatibility with current technology. Here we present the state-of-the-art in the studies of electrical properties of SCO materials. We will start from results obtained on bulk powders and crystals, then reduce the scale to thin films and nanoparticles and associated devices, and finally to single molecules. We aim this review to be exhaustive, which is the main difference with respect to other recent reviews on this topic with more specific scopes [24–26]. It should be noted that conceptually rather similar Prussian blue analogue systems have been also studied recently for their electrical properties [27–31], but we will not embrace this topic in the present review.

2. Macroscopic Samples

The first report on the thermal bistability in the (quasi-static) dielectric constant, *i.e.* the relative dielectric permittivity, as a consequence of the reversible LS↔HS transition was presented in 2003 by Bousseksou *et al.* for a series of spin crossover materials [32]. Figure 1 shows the thermal hysteresis of the dielectric constant associated with the spin transition for the $[Fe(NH_2trz)_3](NO_3)_2$, $Fe[5NO_2\text{-sal-N}(1,4,7,10)]$ and $Fe_{0.8}Ni_{0.2}(btr)_2(NCS)_2 \cdot H_2O$ spin crossover compounds, together with the associated thermal variation of the proportion of the HS molecules measured through magnetic susceptibility and reflectivity measurements. The change in dielectric constant upon the spin transition is due to a large change in electronic polarizabilities caused by the concomitant effect of electronic structure change and local symmetry distortion. Interestingly, it can go both ways: the dielectric constant of the HS state can be either superior (more frequent) or inferior to that of the LS state [33,34]. The transition temperatures measured through dielectric techniques follow the values found by other well-known methods used to study the SCO phenomena (magnetic susceptibility and optical measurements). Moreover, these temperatures are independent of the frequency of the applied field (up to at least 1 MHz), which is characteristic of a system in the absence of electron transfer. Later, in 2006 Bonhommeau *et al.* [35] showed the possibility of switching the dielectric constant of $[Fe(L)(CN)_2] \cdot H_2O$ by light irradiation (where L is a Schiff base macrocyclic ligand). The switching of a SCO material using light involves quantitative trapping of the molecules in the excited HS state (light induced excited spin state trapping, LIESST), which can remain in the metastable state for several days at low temperatures (usually below 50 K). The corresponding change in dielectric constant was attributed, based on density functional theory (DFT) calculations, to different polarizabilities in the LS and the HS states caused by the structural modifications which accompany the spin transition.

The change of the dielectric constant of SCO materials provides perspectives towards the use of these materials in micro/nanoelectronic devices, for example in capacitive memory devices. Nevertheless one must note that the absolute values of the dielectric constant remain moderate in these compounds and the reported changes on the SCO are usually not very high (from a few percent to a few tens of percent).

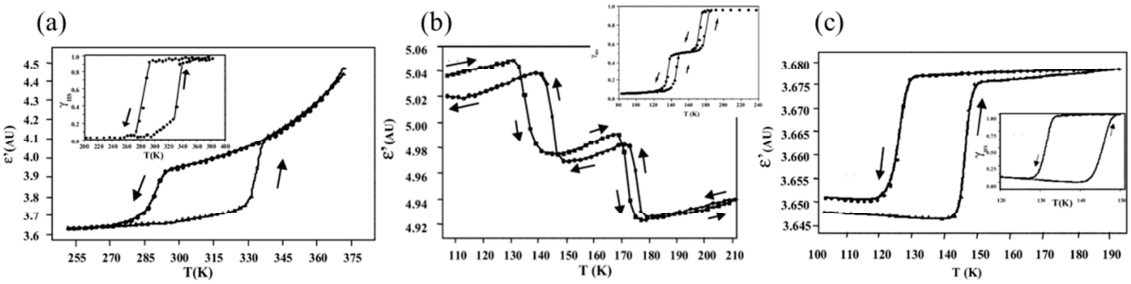

Figure 1. Thermal hysteresis of the dielectric constant associated with the spin transition for the (**a**) $[Fe(NH_2trz)_3](NO_3)_2$; (**b**) $Fe[5NO_2\text{-sal-N}(1,4,7,10)]$ and (**c**) $Fe_{0.8}Ni_{0.2}(btr)_2(NCS)_2 \cdot H_2O$ spin crossover compounds. The insets show the thermal variation of the proportion of the HS molecules measured through (**a**)–(**b**) magnetic susceptibility and (**c**) optical reflectivity measurements. Reprinted from Ref. [32]. with permission from The Royal Society of Chemistry.

From a practical point of view the switching of the electrical conductivity is of significant interest. The first report on the conductivity switching of a bulk SCO solid was published in 2009 [36]. In this work, Salmon *et al.* re-investigated the spin crossover phenomenon in the $[Fe(HB(pz)_3)_2]$ (pz = pyrazolyl) complex by magnetic, calorimetric, optical, crystallographic and electrical means. The magnetic and optical properties revealed irreversible phenomena occurring at the LS to HS transition upon the first heating. This effect has been attributed to a crystallographic change from a tetragonal to a monoclinic structure. During further cycling the magnetic moment displayed a reproducible gradual variation between *ca.* 290 K (LS) and 450 K (HS). Using a broadband dielectric spectrometer the complex conductivity of the sample was also recorded over two consecutive thermal cycles and the irreversible character of the first (magneto-structural) transition was clearly evidenced in the electrical measurements around 410 K where an abrupt, *ca.* 3 orders of magnitude decrease in conductivity was registered. The next thermal cycle followed exactly the conductivity variation of the first cooling curve. Charge hopping process has been proposed as the main transport mechanism for this material with the LS state being more conductive. In the case of $[Fe(HB(pz)_3)_2]$ the analysis of electrical properties was complicated by the simultaneous electronic, crystallographic and morphologic transformations of the sample. A more clear-cut situation is presented by the spin-state dependence of the electrical conductivity of the $[Fe(Htrz)_2(trz)](BF_4)$ (Htrz = 1H-1,2,4-triazole) SCO compound [37]. Different synthesis batches of this complex were analyzed and each sample presented a spin transition with wide hysteresis loops above room temperature, with slightly different transition temperatures depending on their morphology. DC electrical measurements were performed on the powders compacted between two stainless steel electrodes. The conductivity of the samples was rather low, typically between 10^{-8} and 10^{-10} S/cm at room temperature. The electrical conductivity plotted as a function of temperature revealed a clear hysteresis loop for each sample with transition temperatures that correspond to the values found by optical reflectivity measurements. Figure 2a shows an example where a strong thermal activation of the conductivity is observed in the heating mode (LS state) followed by an abrupt (reversible) drop of *ca.* 2 orders of magnitude around 372 K, corresponding to the LS→HS transition. Even if the samples were found systematically more conductive in the LS state, the analysis of thermal activation energies suggested that in some circumstances the opposite behavior might be also expected to occur. The low conductivity and strong thermal activation indicate that the charge transport takes place through a polaron hopping process. In this framework, the change in conductivity upon the spin transition was attributed to a modification of the vibrational frequencies. Indeed, the LS to HS transition is accompanied by a decrease in the phonon frequencies, which is expected to result in a lower charge carrier hopping rate. The charge transport properties of the same compound were further investigated by Lefter *et al.* [38] using broadband dielectric spectroscopy. This study revealed that the spin transition alters all material related electrical parameters (conductivity, permittivity, loss modulus, charge carrier relaxation times, *etc.*). Of particular interest regarding the

charge transport mechanism is the frequency dependence of the conductivity and the loss modulus (Figure 2b,c). The former exhibits a cut-off frequency separating the dc and ac conductivity regimes, while the latter exhibits a loss peak centered on the charge carrier relaxation frequency. A very significant increase of these characteristic frequencies was observed when going from the HS to the LS state providing thus experimental evidence for the higher hopping frequencies in the LS state. The electrical properties of the $[Fe_{1-x}Zn_x(Htrz)_2(trz)](BF_4)$ Zn-diluted series were also investigated [39]. The conductivity of the diluted compounds decreased with 3 (x = 0.26) and 6 (x = 0.43) orders of magnitude, suggesting that the iron ions participate directly in the charge transport process.

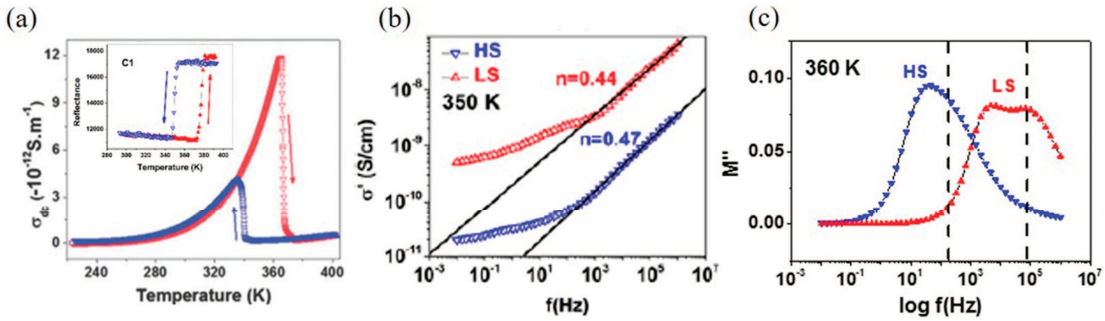

Figure 2. Electrical properties of $[Fe(Htrz)_2(trz)](BF_4)$. (**a**) Temperature dependence of the dc conductivity in the heating and cooling modes. The inset shows the temperature dependence of the high spin fraction; (**b**) Spin state dependence of the conductivity spectra at 350 K; (**c**) Spin-state dependence of the dielectric loss modulus spectra at 360 K. Reprinted from refs. [37] with permission from The Royal Society of Chemistry [38], 2014 WILEY-VCH Verlag GmbH & Co. KGaA©, Weinheim and with permission from [39] Copyright 2015 American Chemical Society.

Overall, bulk SCO solids can be considered as nearly perfect (*i.e.*, low loss) dielectric materials characterized by very low conductivity values. It is thus not surprising that the conductivity changes associated with the SCO have been observed only in samples with spin transitions above room temperature, where the thermal activation allows for raising the conductivity to detectable levels. To overcome this problem several groups attempted to enhance charge transport in SCO compounds by synthesizing hybrid materials comprising both SCO and conducting bricks. This has been achieved both at the microscopic and macroscopic levels.

Hybrid materials containing SCO complexes as well as conducting molecular species in the same crystal lattice were reported by several teams [40–52]. Most of these compounds exhibit either SCO or semiconducting behavior or both at the same time, but (in our opinion) a clearly discernible interplay between the two phenomena has been achieved only in two cases. The first indication of an interplay between the two phenomena were reported in 2006 by Takahashi *et al.* [50]. They synthesized and characterized the $[Fe(qsal)_2][Ni(dmit)_2]_3 \cdot CH_3CN \cdot H_2O$ complex (qsalH = N-(8-quinolyl)-salicylaldimine, dmit = 4,5-dithiolato-1,3-dithiole-2-thione), which presents a gradual spin conversion from room temperature to 120 K in a multi-step process. The electrical resistivity behavior as a function of temperature is characteristic of a semiconductor, with a relatively high value at room temperature (2 S/cm) and presents a hysteresis loop between 90 and 120 K similar to the magnetic measurements. A correlation thus appears between the SCO phenomenon and the electrical conduction, but the complicated temperature dependence of the spin crossover and the lack of structural characterization did not allow for an unambiguous conclusion. A more clear-cut result was later obtained by the same group [51] with the compound $[Fe(qnal)_2][Pd(dmit)_2]_5 \cdot$ acetone [qnalH=N-(8-quinolyl)-2-hydroxy-1-naphthaldimine]. This compound displayed a quasi-complete spin transition around 220 K as shown by the magnetic measurements in Figure 3a. The electrical measurements revealed a rather high conductivity value at room temperature (*ca.* 10^{-2} S/cm), and even more importantly a discontinuity was observed in the temperature dependence of the resistivity

around 220 K, which is in the same range as the spin transition. The activation energy before the resistivity change is 0.37 eV (LS state), while after the "anomaly" the activation energy is 0.24 eV (HS state). Looking at the temperature dependence of the crystal lattice cell parameters shown in Figure 3b, a significant change at 220 K can be observed for the *a* axis. The authors suggested this uniaxial strain might be the origin of the conductance switching upon the SCO.

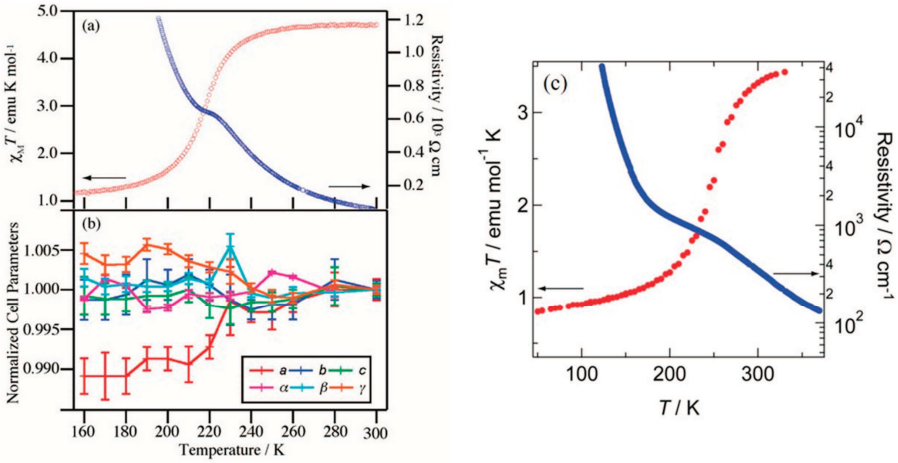

Figure 3. Temperature dependence of (**a**) the $\chi_M T$ product and electrical resistivity and (**b**) the lattice cell parameters (normalized to the values at 300 K) for the compound $[Fe(qnal)_2][Pd(dmit)_2]_5 \cdot$ acetone. (**c**) Temperature dependence of the magnetic susceptibility and electrical resistivity of $[Fe(dppTTF)_2][Ni(mnt)_2]_2(BF_4) \cdot PhCN$. Reprinted with permission from Ref. [51]. Copyright 2008 American Chemical Society. Reproduced from Ref [45] with permission of The Royal Society of Chemistry.

A similar result was obtained by Nihei *et al.* [45] by mixing Fe(II) SCO complexes with tetrathiafulvalene conductive moieties. They synthesized and characterized the compounds $[Fe(dppTTF)_2](BPh_4)_2 \cdot MeNO_2 \cdot 0.5Et_2O$ and $[Fe(dppTTF)_2][Ni(mnt)_2]_2(BF_4) \cdot PhCN$ (dppTTF = 1-{2-(1,3-dithiol-2ylinene)-1,3-dithiolyl}-2-{2,6-bis(1-pyrazolyl)pyridyl}-ethylene, mnt = maleonitriledithiolate). The magnetic susceptibility measurement of the second compound is presented in Figure 3c, wherein a spin crossover around 250 K can be depicted. The electrical measurements performed on a single crystal revealed a rather high conductivity of *ca.* 10^{-3} S/cm at, room temperature and a change in the *R vs. T* slope between 160 K and 280 K, which correspond to the spin crossover region of the complex. In the low temperature region (LS), the activation energy was measured to be 129 meV, while in the high temperature region (HS) the activation energy is 119 meV.

In the previous examples hybrid conducting SCO materials were synthesized by co-crystallization of molecular bricks. This elegant approach offers very interesting prospects from a fundamental point of view, but the synthesis of these compounds is rather challenging. On the other hand, hybrid materials were also obtained at a more macroscopic level by "physically mixing" the constituents. A remarkable synergy between a SCO complex and a piezoresistive polymer has been reported by Koo *et al.* [53] by studying the response of a composite consisting of polypyrrole (PPy) and $[Fe(Htrz)_2(trz)]BF_4$ and/or $[Fe(NH_2\text{-trz})_3]SO_4$ (NH_2-trz = 4-amino-1,2,4-triazole). The composites have been prepared by mixing PPy and the bulk SCO material(s), then pressing at 0.01 GPa to obtain films with thickness greater than 0.05 mm. Electrical measurements where performed using the four probe technique and revealed room temperature conductivity of *ca.* 10^{-2} S/cm. The conductivity as a function of temperature reveals the same hysteresis loop as the magnetic measurements (Figure 4). The HS state is *ca.* 60% more conducting in this sample. In a similar composite containing both $[Fe(NH_2\text{-trz})_3][SO_4]$ and $[Fe(Htrz)_2(trz)][BF_4]$ complexes, the system presents multiple thermal hysteresis and a relative conductivity change as high as 300%. Doped PPy is a highly conductive polymer and, more importantly,

it has piezoresistive properties, *i.e.*, its conductivity changes by applying a pressure. In this case it is assumed that the pressure originates from the mechanical stress and strain associated with the spin transition. (The volumetric strain due to SCO is *ca.* 0.11 in $[Fe(Htrz)_2(trz)]BF_4$.) These results provide important perspectives for obtaining highly conductive plastic films with switching properties at technologically relevant temperatures. We anticipate interesting developments in this direction by promoting synergy between SCO and polymer materials with various electrical properties and promising new functionalities. In particular electro-active polymers are very appealing for the development of SCO-based actuators [23,54,55].

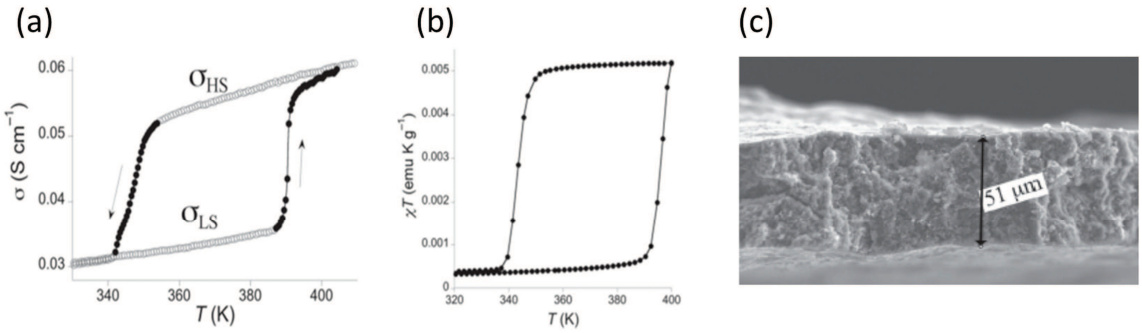

Figure 4. Temperature dependence of (**a**) the electrical conductivity and (**b**) the magnetic properties of a composite consisting of polypyrrole and $[Fe(Htrz)_2(trz)][BF_4]$; (**c**) Electron microscopy image of the film cross-section. Reproduced from Ref. [53], 2014 WILEY-VCH Verlag GmbH & Co. KGaA©, Weinheim.

Hybrid conducting SCO materials have been also fabricated at a truly macroscopic level, by combining SCO polymer composites with electroactive polymers in bilayer structures [54,55]. Chen *et al.* [54] achieved electrical bistability using a bilayer cantilever consisting of a $[Fe(Htrz)_2(trz)](BF_4)$/polycarbonate (PC) composite and a polyimide/constantan alloy/polyimide strain sensitive plate. The temperature dependence of the voltage measured through a Wheatstone bridge presented a hysteresis loop characteristic to the spin transition. It is clear that the measured voltage is related to the metallic conductor not to the SCO/PC composite, however the SCO phenomena is clearly visible through mechanical coupling between the two polymer layers. On the other hand, Gural'skiy *et al.* [55] described an electro-thermomechanical actuator, which consists in a bilayer cantilever combining $[Fe(Htrz)_2(trz)](BF_4)$ with poly(methylmethacrylate) (PMMA) for the first layer and a polymer composite with silver nanoparticles for the second layer. This bilayer cantilever uses the spin crossover phenomenon to convert electrical energy into mechanical motion through Joule heating.

3. Micro- and Nanoscale Devices

Spin crossover thin films and nanoparticles have been integrated recently into electronic devices either to investigate the charge transport properties of the SCO compounds and/or to obtain new device functionalities (switch, memory, *etc.*). Matsuda *et al.* used spin crossover materials to modulate the electroluminescence (EL) of an OLED device ITO/$[Fe(dpp)_2](BF_4)_2$:Chl-a/Al (dpp = 2,6-di(pyrazol-1-yl)pyridine), Chl-a = chlorophyll a). The fluorescent SCO layer was deposited by spin coating on ITO and covered by a thin Al layer in a vertical device configuration. The device presented EL in the HS state, while in the LS state the EL was suppressed (Figure 5a) [56].

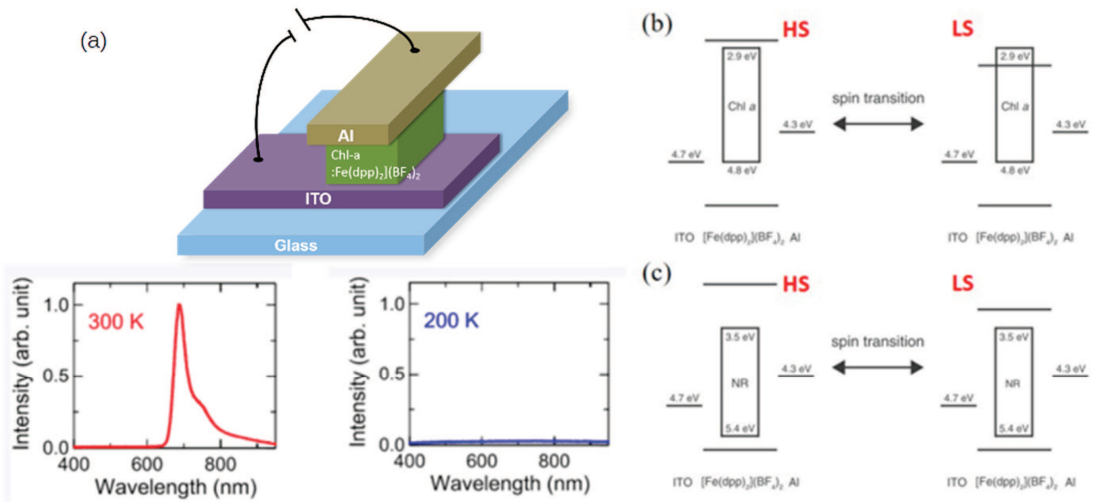

Figure 5. (**a**) Scheme of the OLED device ITO/$[Fe(dpp)_2](BF_4)_2$:Chl-a/Al and its electroluminescence intensity in the HS and LS states; (**b**) and (**c**) Schematic representation of the mechanism proposed for the switching of EL on/off switching upon SCO based on the energy level diagram. (**b**) Energy level diagram for the Chl *a*-doped device with $[Fe(dpp)_2](BF_4)_2$ (**c**) Energy level diagram for the analog NR dye-doped device with $[Fe(dpp)_2](BF_4)_2$. The energy level change in the molecular orbital concerning electron transport accompanying the spin transition regulates electron injection into Chl *a*, but does not affect the electron injection into NR because of its low LUMO level. Adapted with permission from Refs. [56] and [22].

The authors proposed a model where in the LS state the electrons injected from the Al electrode passed through the SCO complex into the ITO electrode, preventing the formation of excited-state Chl-a. [22]. On the other hand, when the SCO material is in the HS state, the electrons and holes combine, therefore EL is registered (Figure 5b). In order to test this hypothesis, a poly(N-vinylcarbazole) (PVK) layer was deposited between the ITO electrode and active layer. PVK is used as a hole transport and electron blocking layer. Indeed the insertion of this layer created an accumulation of charges in the active layer and the EL occurred in both spin states. In a second stage of the experiment, the SCO material was doped with nile red (NR) dye as an emitting dopant instead of Chl-a. In this case also, EL was detected in both spin states, which was explained by the lower lying electron transport orbitals in NR *vs.* Chl-a (Figure 5c).

Mahfoud *et al.* presented the proof of concept for a read-only memory (ROM) containing the $[Fe(HB(pz)_3)_2]$ SCO complex [57]. In this work the complex has been thermally evaporated in thin film form onto interdigitated microelectrodes. The current-voltage (*I-V*) characteristic of the device presents an Ohmic variation, before and after heating the device to 408 K (Figure 6a). This represent the read operation of the device before and after the writing. An all-electrical read-write process is shown in Figure 6b, where different voltage bias has been applied for *ca.* 1 min to the device at 370 K. When a voltage bias of 1 V was applied no effect occurred. This can be considered as the read operation of the ROM. By increasing the voltage to 2 V the measured current decreases abruptly after 40 s and remains at a very low value. This irreversible effect, attributed to a Joule heating induced structural transition in the material, corresponds to the writing of the memory.

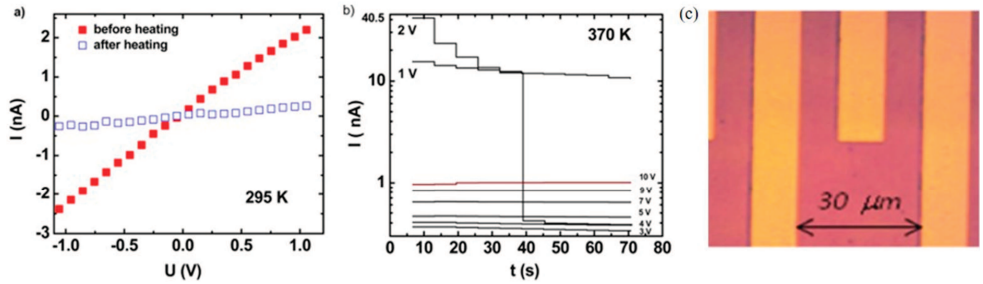

Figure 6. (**a**) Current-voltage characteristic of the ROM device with $[Fe(HB(pz)_3)_2]$ recorded at 295 K before and after heating the device to 408 K; (**b**) Reading and writing process of the ROM device performed at 370 K; (**c**) Optical microscopy picture of the micro-electrodes after the deposition of the $[Fe(HB(pz)_3)_2]$ film. Reprinted with permission from Ref. [57]. Copyright 2011, AIP Publishing LLC.

A somewhat similar process was used to fabricate devices with $Fe(phen)_2(NCS)_2$ (phen = 1,10-phenanthroline) thin films by Shi *et al.* [58]. The temperature dependence of the magnetic susceptibility of a 280 nm thin film revealed an abrupt spin transition at 175 K, similar to the bulk powder sample. For the electrical characterization a thin film of 240 nm has been deposited between gold electrodes and characterized at room temperature. The logarithmic representation of the *I-V* curve revealed two linear regions: one region at low voltages with a slope of 1.17, suggesting Ohmic conduction and a second linear region above 1.4 V with a slope of 2.04 characteristic to space charge limited current regime. From these data a charge carrier mobility of 6.53×10^{-6} $cm^2/V \cdot s$ has been deduced. Temperature-dependent transport measurements were not reported, presumably due to the very low current levels around the spin transition temperature.

The control of the spin state of $[Fe(H_2B(pz)_2)_2(bipy)]$ (where bipy = 2,2′-bipyridine) thin films deposited by thermal evaporation on organic ferroelectric polyvinylidene fluoride with trifluoroethylene P(VDF-TrFE) was demonstrated by Zhang *et al.*, by changing the electric field at the interface of the two layers [59]. Magnetometry studies performed on the thin film stack revealed compelling evidence of voltage control of the spin state of the SCO layer. As a reference, the magnetic properties of the SCO powder are depicted in Figure 7a, showing the paramagnetic HS state at 300 K and the diamagnetic LS state at 100 K. In the case of the thin films (*ca.* 25 molecular layer), the paramagnetic behavior (characteristic to high temperatures) could be measured down to 100 K when the P(VDF-TrFE) film was polarized "up", while the diamagnetic behavior (characteristic to low temperatures) was observed up to room temperature when the ferroelectric film was polarized "down" (Figure 7b).

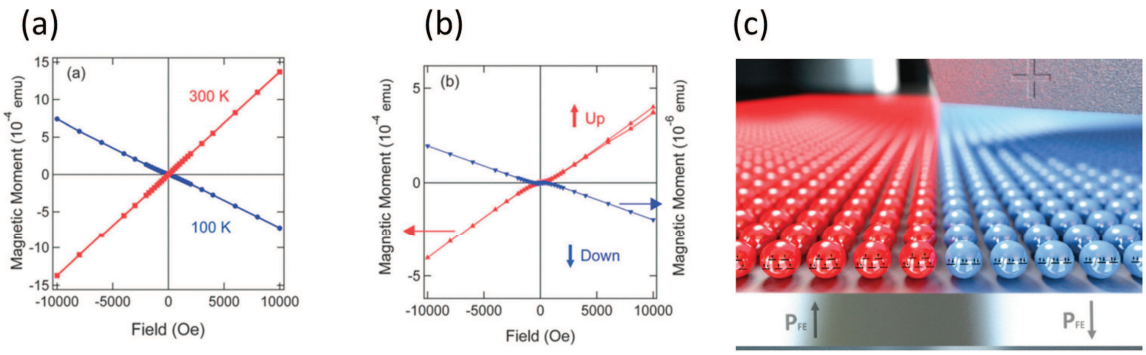

Figure 7. (**a**) Magnetic properties of $[Fe(H_2B(pz)_2)_2(bipy)]$ powder at 100 K (LS) and 300 K (HS); (**b**) Magnetic properties of the films of $[Fe(H_2B(pz)_2)_2(bipy)]$ on the ferroelectric P(VDF-TrFE) substrate for different polarizations. The color chart is a schematic view of the substrate polarization effect. (**c**) Visual representation of the spin state transition upon changing the polarization of the substrate. Reproduced from Ref. [59] with permission of The Royal Society of Chemistry.

Rotaru *et al.* used a different approach wherein micro- and nanoparticles of $[Fe(Htrz)_2(trz)](BF_4)$ have been organized between interdigitated electrodes using dielectrophoresis [60]. The particles were dispersed in ethanol and drop-cast on interdigitated gold electrodes. By applying an ac voltage, the electric field gradient induced in the solution attracted the SCO objects to the gaps between electrodes (Figure 8a,b). By using high aspect ratio particles the orientation order parameter has been drastically improved, reaching $S = 0.86$ (where $S = < 2\cos^2\theta - 1 >$ and θ is the angle between a particular object and the mean orientation of any other object). This value was obtained for particles with 4 µm length and 300 nm in diameter deposited from a 0.2 g/L suspension using 7 V_{rms} and 10 kHz ac bias for dielectrophoresis. The temperature dependence of the measured current (Figure 8c) revealed a similar behavior as that obtained for the powder sample (see Figure 2a), *i.e.*, the device presents a wide thermal hysteresis loop centered around 370 K with the LS state being more conductive. The *I-V* characteristics recorded at 373 K in both spin states showed a non-linear behavior, which probably originates in a voltage activation of the charge transport. Overall, fairly similar results were reported later by Dugay *et al.* [61] for $[Fe(Htrz)_2(trz)](BF_4)$ nanoparticles integrated in a similar device. Lefter *et al.* [62] completed the study of $[Fe(Htrz)_2(trz)](BF_4)$ based devices by the analysis of the robustness of the thermal spin transition and that of the electronic device on successive thermal cycling. While the powder showed a fairly good stability up to 3000 thermal cycles in optical reflectivity measurements, the current intensity dropped monotonously in electrical measurements over 20 cycles, even if the spin transition temperatures were reproducible.

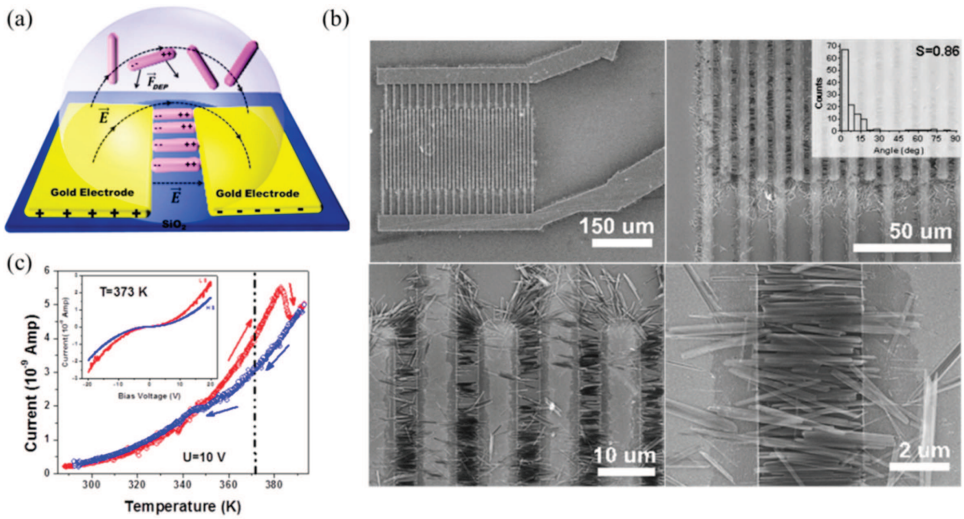

Figure 8. (**a**) Schematic representation of the dielectrophoresis process used to align $[Fe(Htrz)_2(trz)](BF_4)$ particles between electrodes; (**b**) SEM images of a device with the insert showing the orientation order parameter; (**c**) Temperature dependence of the measured current in the device over a heating-cooling cycle under 10 V bias. Inset: I-V characteristic recorded at 373 K in the LS and HS states. Reproduced from Ref. [60], 2014 WILEY-VCH Verlag GmbH & Co. KGaA©, Weinheim.

Photoconductivity experiments on $[Fe(Htrz)_2(trz)](BF_4)$ micrometric rods were also carried out [63]. The rods where placed between interdigitated gold electrodes and light form a halogen lamp was applied on the device inside the hysteresis temperature range. A significant decrease in current upon light irradiation was observed in the LS state. This phenomenon has been tentatively attributed to charge trapping caused by adsorbed molecules from the ambient atmosphere, but the origin of the spin-state dependence could not be clarified. More recently, the possibility of a partial switching of the spin state of $[Fe(Htrz)_2(trz)](BF_4)$ particles from the HS to the LS state by applying an electrical field was also reported [64]. Another interesting effect has been observed by Etrillard *et al.* [65] on the photoconduction in $[Fe(Htrz)_2(trz)](BF_4)\cdot H_2O$ nanocrystals, which have been positioned between sub 100 nm gap gold electrodes. The particles were randomly dispersed on the substrate from an ethanol

solution and effectively bridged the gap between electrodes. A first experiment has been performed on the as-prepared device and no photocurrent has been measured. Then the electrodes where subjected to voltage poling. The current of the poled device increased considerably upon light irradiation and dropped to the same level when the light excitation was removed. Even though the experimental results are intriguing, it is not clear if the effect is characteristic of the SCO material.

One of the most intriguing results on electrical properties of SCO materials was reported by Prins *et al.* [66] where they showed the possibility of addressing a SCO nanoparticle. The SCO system is formed of $[Fe(Htrz)_2(trz)][BF_4]$ nanoparticles coated with a surfactant shell. The particles were deposited between gold electrodes with an electrode gap of 5–10 nm as it is schematically illustrated in Figure 9a. The current-voltage characteristics (Figure 9b) show the difference before (green line) and after (red line) particle deposition by a clear increase in the measured current for two different devices (electrode width of 1 μm and 100 nm respectively). Multiple *I-V* characteristics where recorded at different temperatures in the temperature range of 300-400 K and by plotting the conductance (I/V) of the device at 0.4 V as a function of temperature, a hysteretic behavior similar to the one obtained in the magnetic susceptibility measurements was found (Figure 9c). It is important to note that in both devices the conductance in the HS state is several times higher than the conductance in the LS state, which is exactly the opposite behavior with respect to the bulk material. The switching between the low-conductance and higher conductance states was also achieved by voltage cycling (Figure 9d). The authors suggested that the origin of this conductance difference could be the expansion of the Fe–N bond length that accompanies the spin transition. By assuming a single electron tunneling phenomena in the device, the increase in bond length upon the spin transition can reduce the tunnel barrier width, thus leading to an increase of the conductance.

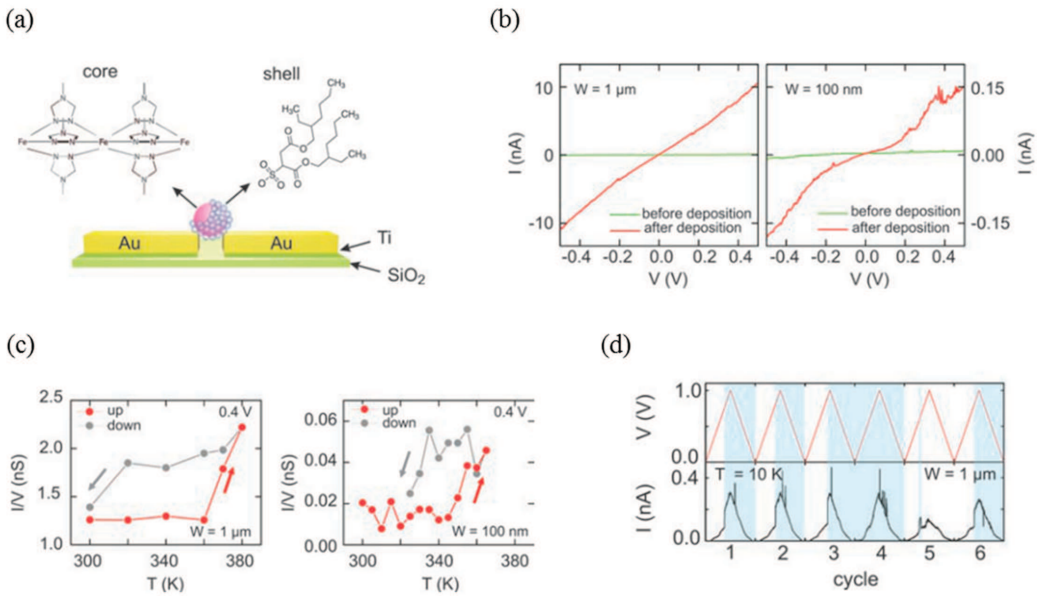

Figure 9. (**a**) Schematic representation of a device with surfactant coated $[Fe(Htrz)_2(trz)](BF_4)$ nanoparticles in the electrode gap; (**b**) Current-voltage characteristic of two different devices (with an electrode width of 1 μm and 100 nm respectively) recorded before and after particle deposition; (**c**) Temperature dependence of the conductance plotted for 0.4 V bias; (**d**) Conductance switching (1 μm device) using a triangular voltage at 10 K. Reproduced from Ref. [66], 2014 WILEY-VCH Verlag GmbH & Co. KGaA©, Weinheim.

4. Single Molecule Studies

As a matter of fact, the above mentioned work of Prins *et al.* [66] on single SCO nanoparticles represents an intermediate situation between the investigation of SCO materials and single SCO

molecules. These latter have been recently studied by several groups using either scanning tunneling microscopy (STM) or planar, two- or three terminal, "nanogap devices". Working with such single-molecule electronic and spintronic devices is obviously a very attractive and challenging topic. Nevertheless, a word of caution is necessary for the spin crossover community as to the interpretation of the data obtained by these techniques. In most cases there is only *indirect* evidence for the spin-state switching in these devices. From a fundamental point of view, the main issue is that the connection of the molecules to the electrodes will *always* alter their properties to some extent. Hence a direct comparison with the bulk properties often becomes meaningless. From a practical point of view the key problem is that the experimental characterization of the molecule in the junction is nearly impossible by any other means than the tunneling current. From this point of view STM offers somewhat more flexibility than nanogaps, nevertheless, a series of carefully controlled experiments and theoretical calculations are indispensable in each case to rationalize the observations.

The first STM study on a SCO compound was published by Alam *et al.* [67] who investigated the $[Fe^{II}(L)_2](BF_4)_2$ (L = 2,6-di(1H-pyrazol-1-yl)-4-(thiocyanato-methyl)pyridine) complex. The compound has been deposited from solution on highly oriented pyrolytic graphite (HOPG) surfaces for current-imaging tunneling spectroscopy (CITS). This technique has been used to map the nanometric chain structures formed on the surface. Two different types of molecular clusters were observed with I-V curves situated either higher or lower than the reference curve of the HOPG surface. The two types of signals were attributed to LS molecules (more conductive) and HS molecules, respectively. The study of $[Fe^{II}(L')_2](X)_2$ complexes was completed later by Grohmann *et al.* [68]. In this article they studied two complexes with L′ = 2,6-di(1H-pyrazol-1-yl)pyridine and X = BF_4 and X = PF_6. In the bulk polycrystalline form, only the former exhibits spin crossover, while the latter is a high spin complex. However, the I-V characteristics of both complexes deposited on the HOPG surface present different features, which could be assigned to the coexistence of HS and LS molecules on the surface.

An interesting perspective has been published by Palamarciuc *et al.* by performing STM imaging on isolated molecules of the $[Fe(H_2B(pz)_2)_2(bipy)]$ SCO complex obtained by evaporation on a Cu(111) surface [69]. They observed a series of isolated molecules with different orientations from which they deduced the possible adsorbate conformation of the molecule on the surface. The same family of compounds has been also investigated by other groups. Pronschinske *et al.* [70] studied by STM bilayer $[Fe(H_2B(pz)_2)_2(bipy)]$ films on Au(111) surfaces and observed in the conductance maps the coexistence of two different molecules, but no significant temperature effect between 130 and 300 K on the relative population of the two species. From a comparison of the tunneling spectra and DFT calculations they concluded on a temperature independent coexistence of molecules in the two spin states, the HS state exhibiting a reduced conductance gap with respect to the LS state. The STM investigation of the closely related compound $[Fe(H_2B(pz)_2)_2(phen)]$ on Au(111) has been presented by Gopakumar *et al.* [71]. Remarkably, they showed a reversible and selective switching of single molecules in a densely packed bilayer of molecules by injecting electrons from the STM tip. The switching process involved a significant change of the differential conductance spectra and showed correlation with DFT calculations, indicating in both cases (*i.e.*, theory and experiment) a decreased gap between the highest-occupied and lowest-occupied molecular orbitals (HOMO-LUMO). In addition a Kondo resonance was also reported in the "reduced gap" molecular state. On this basis the observed switching process was described as a transition between the LS and HS states.

The operation of a nanoscale molecular switch containing a single molecule to store information has been presented by Miyamachi *et al.* [72]. In this work they studied $Fe(phen)_2(NCS)_2$ spin crossover molecules deposited on metallic surfaces and they observed a field-induced switch between a low and high conduction state. Remarkably this switch could be obtained only when the molecules were decoupled from the metallic substrate by a nitrogen insulating layer—highlighting the outmost importance of the electronic coupling between the molecules and the substrate. The hysteretic *I-V* characteristic of a single molecule is presented in Figure 10a.

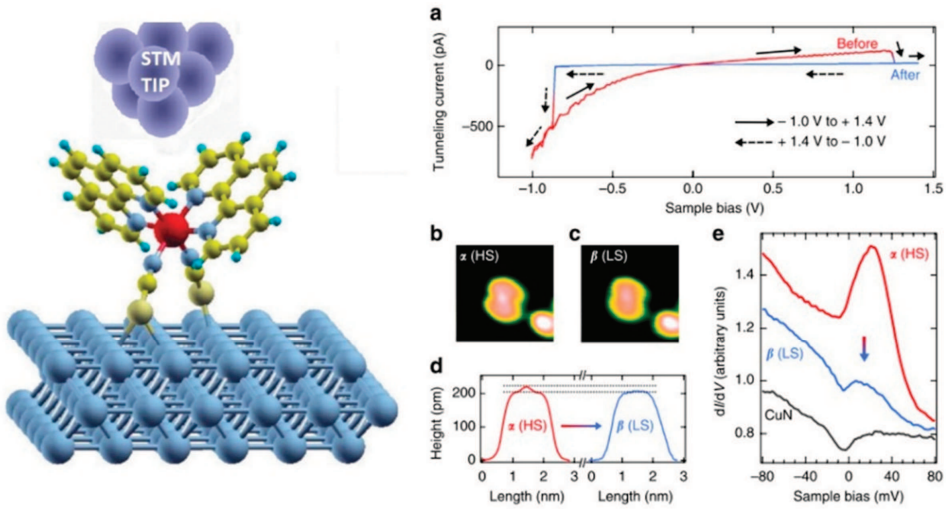

Figure 10. (**a**) *I-V* characteristic of an isolated $Fe(phen)_2(NCS)_2$ molecule on CuN/Cu(100) surface. STM image for the (**b**) HS and (**c**) LS states with the corresponding (**d**) height profile; (**e**) Differential conductivity of the molecule in the HS and LS states as well as that of the CuN insulating layer. Reprinted with permission from ref. [72].

The higher and lower conduction states can be obtained reversibly by applying a bias of +1.2 V and −0.8 V, respectively. The switching of the tunneling current with the bias ramping is also accompanied by a structural change observed in the STM images as well as in the height profiles as shown in Figure 10. The difference between the two states can be highlighted by plotting the differential conductance (dI/dV) as illustrated in Figure 10e. The difference between the two states is clear here, as only one of the two states shows a Kondo peak, characteristic of a magnetic impurity on a conductive surface. On this basis the high (low) conductance state is assigned to the HS (LS) state of the molecule. This switching phenomenon has been also used to demonstrate a memristor operation in these devices. Gruber *et al.* [73] continued the work on the same complex deposited on Cu(100) surface with coverages ranging from 0.1 to 1.8 monolayers on which STM measurements where performed. A coverage-independent coexistence of both spin states at low temperatures (4 K) on the first monolayer has been reported. In the case of the second-layer molecules, the influence of the substrate is reduced and a switching between the two states was observed when cycling the bias voltage. Gueddida *et al.* [74] have calculated by DFT the STM pictures of $Fe(phen)_2(NCS)_2$ on transition metal surfaces and pointed out the importance of electronic coupling with the substrate.

The low temperature charge transport mechanism in a three terminal device containing a Mn-transition metal complex ($[Mn(terpy\text{-}O\text{-}(CH_2)_6\text{-}SAc)_2)]^{2+}$) has been studied by Osorio *et al.* [75]. Using this configuration the authors demonstrated the direct electrical control of the molecular spin state of a single metal complex. To this aim the molecule was bonded to two gold electrodes obtained by electromigration. By adjusting the gate-voltage the terpyridine ligand was reduced leading to an increase of the ligand-field on the central metal ion, which allowed for a transition between the $S = 5/2$ and $S = 1/2$ spin states of the molecule. A more comprehensive study has been presented by Meded *et al.* [76] where they show theoretically and experimentally the possibility of electrically controlling the spin-state of a single molecule. Using DFT calculations they predicted that the spin transition can be triggered when two electrons are added to the ligands in the complex $[Fe^{II}(bpp)_2]^{2+}$ [bpp: 2,6-bis(pyrazol-1-yl)pyridine]. From an experimental point of view they used a three-terminal device configuration with a single molecule of the $[Fe\text{-}(L)_2]^{2+}$] complex [L = 4′-(4‴-pyridyl)-1,2′:6′1″-bis-(pyrazolyl)pyridine] as shown in Figure 11a. Figure 11b illustrates a typical differential conductance map as a function of the source-drain and gate voltages, which exhibits a classical single-electron transport trough a nano-object. The shift in the gate voltage ΔV_g of the Coulomb edges is a consequence of the modification of the electrostatic environment of the

molecule. These transport measurements reveal a double-quantum-dot behavior combined with a split Kondo peak, which can be interpreted as an indication of an SCO behavior.

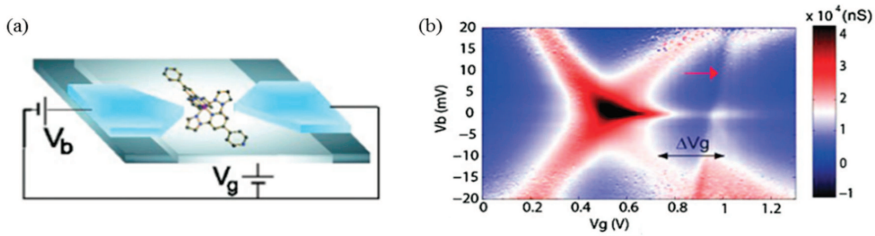

Figure 11. (**a**) Schematic representation of the three-terminal device containing a SCO molecule; (**b**) Differential conductance as a function of source-drain (V_b) and gate (V_g) voltages. Reprinted with permission from Meded, V.; Bagrets, A.; Fink, K.; Chandrasekar, R.; Ruben, M.; Evers, F.; Bernand-Mantel, A., Physical Review B, 83, 245415, 2011. Copyright 2011 by the American Physical Society.

The spin crossover phenomena and the charge transport properties at the single molecule level have been studied recently by two different approaches: by grafting SCO molecules to an array of gold nanoparticles [77] and also by means of mechanically controlled break junctions [78].

In the first case the complex studied was $[Fe(AcS\text{-}BPP)_2](ClO_4)_2$, where AcS-BPP = (S)-(4-[[2, 6-(dipyrazol-1-yl)pyrid-4-yl]ethynyl]phenyl)ethanethioate). Molecules were attached to gold nanoparticles of 8.5 nm in diameter, which were then arranged in a 2D network, as shown in Figure 12. The particular interest of such well-organized molecule-nanoparticle networks is that the occurrence of SCO phenomena in the junctions could be confirmed by independent control techniques (Raman spectroscopy and magnetization measurements). Charge transport measurements as a function of temperature have been performed on four devices, three of which contained passive "control" molecules. Figure 12 shows the temperature dependence of the resistance of a few devices. The monotonic decrease of the resistance and the formation of the plateau at higher temperatures is an indication of a Coulomb blockade due to the small size of the nanoparticles. This was observed for each device. On the other hand an increase of resistance above 280 K was observed only in the case of the SCO-gold nanoparticle arrays. The charge transport behavior of the device containing SCO molecules was explained through a percolation model that assumes that the HS state is more resistive than the LS state, assumption that has been confirmed also by theoretical calculations.

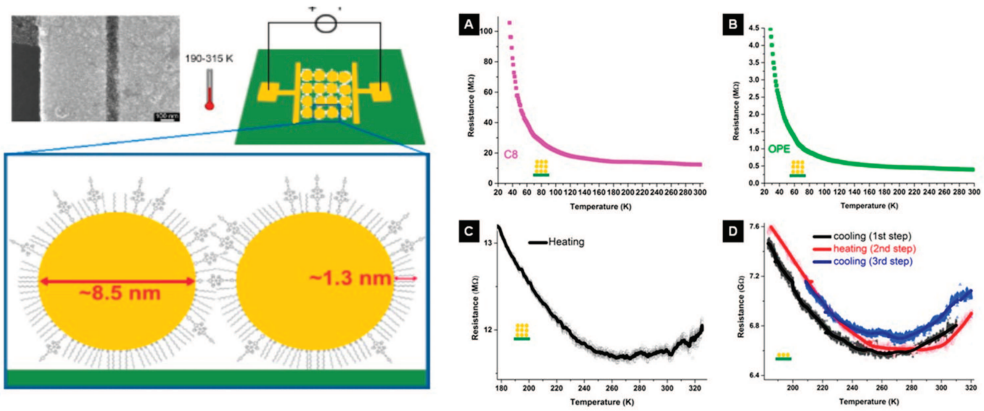

Figure 12. Left panel: SEM image and schematic drawing of the SCO molecule—gold nanoparticle 2D array used in ref. [77] for single molecule conductance studies. Right panel: Resistance as a function of temperature of a gold nanoparticle network with (**A**) octanethiol molecules; (**B**) dithiolated oligo(phenylene ethynylene) molecules; (**C**) SCO molecules (three layers) and (**D**) SCO molecules (monolayer). Reprinted with permission from Ref. [77] Copyright 2015 American Chemical Society.

Spin state switching using a voltage of a single [$Fe^{II}(tpy)_2$] molecule placed in a mechanically controlled break junction has been demonstrated by Harzmann *et al.* [78]. This experiment is based on the sensitivity of spin state of this complex to the spatial arrangement of the ligands. By applying an electric field across the molecule, a mechanical distortion of the coordination sphere occurs leading to a change of the ligand field. A schematic representation is shown in Figure 13. The experimentally observed typical *I-V* characteristics are also illustrated in Figure 13. The three main *I-V* characteristics found in 28 devices are as follows. In four of them a hysteretic behavior has been observed, displaying a current jump at 0.7 V upon sweeping forward and a second jump at −0.5 V by sweeping in the opposite direction (Figure 13a). In the remaining 24 junctions a negative differential conductance (Figure 13b) or current jumps (Figure 13c) have been recorded in both sweeping directions. This variety of characteristics may be the result of different orientations of the molecule in the junction with various extents of electrode-molecule interactions.

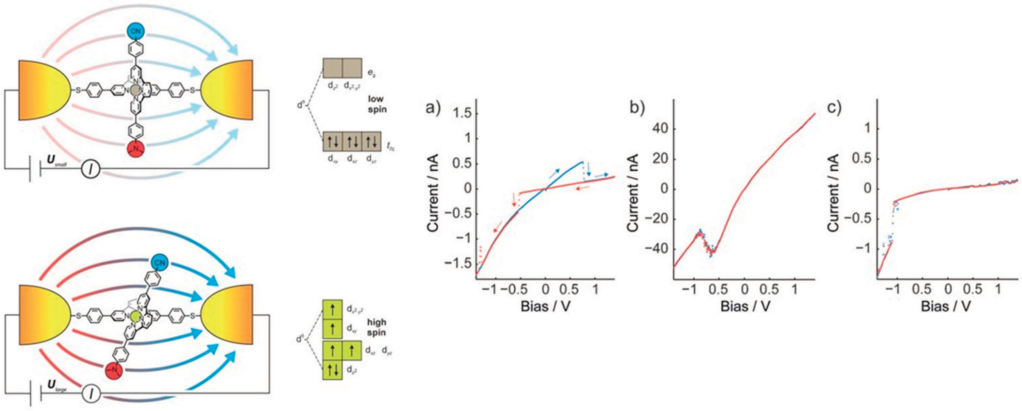

Figure 13. Schematic representation of the voltage triggered spin transition of the [$Fe^{II}(tpy)_2$] complex. *I-V* characteristic showing (**a**) hysteresis; (**b**) negative differential conductance and (**c**) a jump in current. Reproduced from Ref. [78], 2015Wiley-VCH Verlag GmbH &Co. KGaA©, Weinheim.

The change of the resistance of single SCO molecules connected to metallic electrodes has been theoretically studied by Baadji and Sanvito [79] using a combination of density functional theory and the non-equilibrium Green's function methods for quantum transport. They have determined a magnetoresistance ratio of 200% at zero bias and around 3000% at higher voltage biases. The simulated *I-V* characteristic showed a current intensity difference between the HS and the LS states of three orders of magnitude. In the LS state the current has a tunnel-like characteristic in the whole voltage range and increases monotonically with bias. In the HS state, however, the *I-V* characteristic is different since a relatively small voltage bias as 0.4 V is enough to shift both the HOMO and the LUMO transmission resonances within the bias window. These results not only prove that the molecule in the two spin states possesses very different conductivities, but also that the mechanism of the molecular switching is not only associated to a change in the molecule geometry, but has an electronic origin as well. A similar theoretical approach has been adopted by Aravena *et al.* [80] to compute the *I-V* characteristics of a trans-bis(3-(2-pyridyl)[1,2,3]triazolo[1,5-a]-pyridine)bis(isothiocyanato)iron(II) molecule connecting two gold electrodes. They predicted a higher current in the HS state with respect to the LS state and made some comparisons with the available experimental data as well.

5. Conclusions

In this review, we assessed the achievements in the field of spin crossover complexes concerning their charge transport and electrical properties. Starting from the pioneering works on the bistability of the dielectric constant of bulk SCO powders to the voltage-triggered spin transition in a single molecule, this field has advanced considerably in the past decade. At the macroscopic scale the spin-state dependence of charge transport and dielectric properties offers new opportunities

for the investigation of the charge carrier dynamics and electronic structure of these compounds. In addition, these properties open up perspectives for the development of micro- and nano-electronic devices with spin-state switching functionality. The highly insulating nature of SCO compounds represents, however, an obstacle for a number of applications. This problem has been overcome by the development of hybrid SCO-conductor systems, which can also give rise to interesting synergies between different electronic phenomena. Hybrid materials were first synthesized by the co-crystallization of molecular SCO and conductor units, which proved to be a fundamentally very interesting, but also a very challenging synthetic task. In a more pragmatic manner, SCO complexes were also mixed with piezoresistive polymers, which lead eventually to bistable conducting composite materials. We anticipate in the near future a significant further development of this promising approach using polymer matrices with different electrical properties. Other possible approaches to overcome the insulating nature of SCO compounds are based on the device design. For example devices with different competing charge transport channels can be constructed wherein the spin crossover phenomenon can lead to a switching between these channels. Another interesting possibility is the fabrication of devices with large-area thin SCO junctions (either tunneling or injection-limited), which may open up also prospects for spintronic devices. Another field in fast development is the study of charge transport in SCO complexes at the single molecule level. In the case of single molecule devices, it has been shown that the coupling between the SCO molecule and the metallic electrode has a major impact on the electronic structure and switching properties of the molecule. Nevertheless, by carefully controlling this interface, remarkable results have been presented on single molecules or molecular clusters—including also their electrical addressing. Further work will be, however, necessary to clarify the microscopic details of the different phenomena reported at the single molecule level. Rigorous theoretical simulations will have a major role in this context.

Acknowledgments: This work was founded by the joint French-Romanian project ANR-UEFISCDI, contracts No. 9RO-FR/01.02.2013 and ANR-12-IS07-0003-01. CL thanks to the French Ministry of Foreign Affairs for an Eiffel scholarship.

Conflicts of Interest: The authors declare no conflict of interest.

References

1. Rohrer, H. Limits and possibilities of miniaturization. *Jpn. J. Appl. Phys.* **1993**, *32*, 1335. [CrossRef]
2. Peercy, P.S. The drive to miniaturization. *Nature* **2000**, *406*, 1023–1026. [CrossRef] [PubMed]
3. Keyes, R.W. Fundamental limits of silicon technology. *Proc. IEEE* **2001**, *89*, 227–239. [CrossRef]
4. Jan van der Molen, S.; Liljeroth, P. Charge transport through molecular switches. *J. Phys. Condens. Matter* **2010**, *22*, 133001. [CrossRef] [PubMed]
5. Tsutsui, M.; Taniguchi, M. Single molecule electronics and devices. *Sensors* **2012**, *12*, 7259–7298. [CrossRef] [PubMed]
6. Sanvito, S. Molecular spintronics. *Chem. Soc. Rev.* **2011**, *40*, 3336–3355. [CrossRef] [PubMed]
7. Kahn, O. *Molecular Magnetism*; wiley-VCH: New York, NY, USA, 1993.
8. De Silva, P.A.; Gunaratne, N.H.Q.; McCoy, C.P. A molecular photoionic and gate based on fluorescent signalling. *Nature* **1993**, *364*, 42–44. [CrossRef]
9. Raymo, F.M. Digital processing and communication with molecular switches. *Adv. Mater.* **2002**, *14*, 401–402. [CrossRef]
10. Collier, C.P.; Wong, E.W.; Belohradsky, M.; Raymo, F.M.; Stoddart, J.F.; Kuekes, P.J.; Williams, R.S.; Heath, J.R. Electronically configurable molecular-based logic gates. *Science* **1999**, *285*, 391–394. [CrossRef] [PubMed]
11. Bogani, L.; Wernsdorfer, W. Molecular spintronics using single-molecule magnets. *Nat. Mater.* **2008**, *7*, 179–186. [CrossRef] [PubMed]
12. Gutlich, P.; Goodwin, H.A. *Topics in Current Chemistry. Spin Crossover in Transition Metal Compounds I-III*; Springer-Verlag: Berlin, Germany, 2004.
13. Bousseksou, A.; Molnar, G.; Salmon, L.; Nicolazzi, W. Molecular spin crossover phenomenon: Recent achievements and prospects. *Chem. Soc. Rev.* **2011**, *40*, 3313–3335. [CrossRef] [PubMed]

14. Gutlich, P.; Hauser, A.; Spiering, H. Thermal and optical switching of iron(ii) complexes. *Angew. Chem. Int. Ed. Engl.* **1994**, *33*, 2024–2054. [CrossRef]
15. Spiering, H.; Boukheddaden, K.; Linares, J.; Varret, F. Total free energy of a spin-crossover molecular system. *Phys. Rev. B* **2004**, *70*, 184106. [CrossRef]
16. McCusker, J.K.; Walda, K.N.; Dunn, R.C.; Simon, J.D.; Magde, D.; Hendrickson, D.N. Sub-picosecond. Delta.S = 2 intersystem crossing in low-spin ferrous complexes. *J. Am. Chem. Soc.* **1992**, *114*, 6919–6920. [CrossRef]
17. Letard, J.F.; Guionneau, P.; Goux-Capes, L. Towards spin crossover applications. In *Spin Crossover in Transition Metal Compounds III*; Springer-Verlag: Berlin, Germany, 2004; Volume 235, pp. 221–249.
18. Kahn, O.; Martinez, C.J. Spin-transition polymers: From molecular materials toward memory devices. *Science* **1998**, *279*, 44–48. [CrossRef]
19. Linares, J.; Codjovi, E.; Garcia, Y. Pressure and temperature spin crossover sensors with optical detection. *Sensors* **2012**, *12*, 4479–4492. [CrossRef] [PubMed]
20. Bartual-Murgui, C.; Akou, A.; Thibault, C.; Molnar, G.; Vieu, C.; Salmon, L.; Bousseksou, A. Spin-crossover metal-organic frameworks: Promising materials for designing gas sensors. *J. Mater. Chem. C* **2015**, *3*, 1277–1285. [CrossRef]
21. Salmon, L.; Molnar, G.; Zitouni, D.; Quintero, C.; Bergaud, C.; Micheau, J.C.; Bousseksou, A. A novel approach for fluorescent thermometry and thermal imaging purposes using spin crossover nanoparticles. *J. Mater. Chem.* **2010**, *20*, 5499–5503. [CrossRef]
22. Matsuda, M.; Kiyoshima, K.; Uchida, R.; Kinoshita, N.; Tajima, H. Characteristics of organic light-emitting devices consisting of dye-doped spin crossover complex films. *Thin Solid Films* **2013**, *531*, 451–453. [CrossRef]
23. Shepherd, H.J.; Gural'skiy, I.A.; Quintero, C.M.; Tricard, S.; Salmon, L.; Molnár, G.; Bousseksou, A. Molecular actuators driven by cooperative spin-state switching. *Nat. Commun.* **2013**, *4*. [CrossRef] [PubMed]
24. Ruiz, E. Charge transport properties of spin crossover systems. *Phys. Chem. Chem. Phys.* **2014**, *16*, 14–22. [CrossRef] [PubMed]
25. Gaspar, A.B.; Ksenofontov, V.; Seredyuk, M.; Gutlich, P. Multifunctionality in spin crossover materials. *Coord. Chem. Rev.* **2005**, *249*, 2661–2676. [CrossRef]
26. Sato, O.; Li, Z.-Y.; Yao, Z.-S.; Kang, S.; Kanegawa, S. Multifunctional materials combining spin-crossover with conductivity and magnetic ordering. In *Spin-Crossover Materials*; John Wiley & Sons Ltd: Hoboken, NJ, USA, 2013; pp. 303–319.
27. Sato, O.; Kawakami, T.; Kimura, M.; Hishiya, S.; Kubo, S.; Einaga, Y. Electric-field-induced conductance switching in feco prussian blue analogues. *J. Am. Chem. Soc.* **2004**, *126*, 13176–13177. [CrossRef] [PubMed]
28. Molnar, G.; Cobo, S.; Mahfoud, T.; Vertelman, E.J.M.; van Koningsbruggen, P.J.; Demont, P.; Bousseksou, A. Interplay between the charge transport phenomena and the charge-transfer phase transition in $Rb_xMn_{1-x}Fe(CN)_{6(y)}.H_2O$. *J. Phys. Chem. C* **2009**, *113*, 2586–2593. [CrossRef]
29. Mahfoud, T.; Molnar, G.; Bonhommeau, S.; Cobo, S.; Salmon, L.; Demont, P.; Tokoro, H.; Ohkoshi, S.I.; Boukheddaden, K.; Bousseksou, A. Electric-field-induced charge-transfer phase transition: A promising approach toward electrically switchable devices. *J. Am. Chem. Soc.* **2009**, *131*, 15049–15054. [CrossRef] [PubMed]
30. Ohkoshi, S.-I.; Nuida, T.; Matsuda, T.; Tokoro, H.; Hashimoto, K. The dielectric constant in a thermal phase transition magnetic material composed of rubidium manganese hexacyanoferrate observed by spectroscopic ellipsometry. *J. Mater. Chem.* **2005**, *15*, 3291–3295. [CrossRef]
31. Ohkoshi, S.-I.; Tokoro, H.; Matsuda, T.; Takahashi, H.; Irie, H.; Hashimoto, K. Coexistence of ferroelectricity and ferromagnetism in a rubidium manganese hexacyanoferrate. *Angew. Chem. Int. Ed. Engl.* **2007**, *46*, 3238–3241. [CrossRef] [PubMed]
32. Bousseksou, A.; Molnar, G.; Demont, P.; Menegotto, J. Observation of a thermal hysteresis loop in the dielectric constant of spin crossover complexes: Towards molecular memory devices. *J. Mater. Chem.* **2003**, *13*, 2069–2071. [CrossRef]
33. Guillon, T.; Bonhommeau, S.; Costa, J.S.; Zwick, A.; Letard, J.-F.; Demont, P.; Molnar, G.; Bousseksou, A. On the dielectric properties of the spin crossover complex $Fe(bpp)_2(BF_4)_2$. *Phys. Status Solidi Appl. Mater. Sci.* **2006**, *203*, 2974–2980. [CrossRef]
34. Guillon, T.; Salmon, L.; Molnar, G.; Zein, S.; Borshch, S.; Bousseksou, A. Investigation of the two-step spin crossover complex Fe[5-NO_2-sal-(1,4,7,10)] using density functional theory. *J. Phys. Chem. A* **2007**, *111*, 8223–8228. [CrossRef] [PubMed]

35. Bonhommeau, S.; Guillon, T.; Daku, L.M.L.; Demont, P.; Costa, J.S.; Letard, J.F.; Molnar, G.; Bousseksou, A. Photoswitching of the dielectric constant of the spin-crossover complex $[Fe(L)(CN)_2].H_2O$. *Angew. Chem. Int. Ed. Engl.* **2006**, *45*, 1625–1629. [CrossRef] [PubMed]
36. Salmon, L.; Molnar, G.; Cobo, S.; Oulie, P.; Etienne, M.; Mahfoud, T.; Demont, P.; Eguchi, A.; Watanabe, H.; Tanakae, K.; *et al*. Re-investigation of the spin crossover phenomenon in the ferrous complex $[Fe(HB(pz)_3)_2]$. *New J. Chem.* **2009**, *33*, 1283–1289. [CrossRef]
37. Rotaru, A.; Gural'skiy, I.Y.A.; Molnar, G.; Salmon, L.; Demont, P.; Bousseksou, A. Spin state dependence of electrical conductivity of spin crossover materials. *Chem. Commun.* **2012**, *48*, 4163–4165. [CrossRef] [PubMed]
38. Lefter, C.; Gural'skiy, I.A.; Peng, H.; Molnár, G.; Salmon, L.; Rotaru, A.; Bousseksou, A.; Demont, P. Dielectric and charge transport properties of the spin crossover complex $[Fe(Htrz)_2(trz)](BF_4)$. *Phys. Status Solidi RRL Rapid Res. Lett.* **2014**, *8*, 191–193. [CrossRef]
39. Lefter, C.; Tricard, S.; Peng, H.; Molnár, G.; Salmon, L.; Demont, P.; Rotaru, A.; Bousseksou, A. Metal substitution effects on the charge transport and spin crossover properties of $[Fe_{1-x}Zn_x(Htrz)_2(trz)](BF_4)$ (trz = triazole). *J. Phys. Chem. C* **2015**, *119*, 8522–8529. [CrossRef]
40. Nakano, M.; Fujita, N.; Matsubayashi, G.E.; Mori, W. Modified chesnut model for spin-crossover semiconductors $[Fe(acpa)_2](tcnq)_n$. *Mol. Cryst. Liq. Cryst.* **2002**, *379*, 365–370. [CrossRef]
41. Faulmann, C.; Dorbes, S.; de Bonneval, W.G.; Molnar, G.; Bousseksou, A.; Gomez-Garcia, C.J.; Coronado, E.; Valade, L. Towards molecular conductors with a spin-crossover phenomenon: Crystal structures, magnetic properties and mossbauer spectra of $[Fe(salten)mepepy][M(dmit)_2]$ complexes. *Eur. J. Inorg. Chem.* **2005**, 3261–3270. [CrossRef]
42. Dorbes, S.; Valade, L.; Real, J.A.; Faulmann, C. $Fe(sal(2)\text{-}trien)Ni(dmit)_2$: Towards switchable spin crossover molecular conductors. *Chem. Commun.* **2005**, 69–71. [CrossRef] [PubMed]
43. Faulmann, C.; Dorbes, S.; Lampert, S.; Jacob, K.; de Bonneval, B.G.; Molnar, G.; Bousseksou, A.; Real, J.A.; Valade, L. Crystal structure, magnetic properties and mossbauer studies of $[Fe(qsal)_2][Ni(dmit)_2]$. *Inorg. Chim. Acta* **2007**, *360*, 3870–3878. [CrossRef]
44. Takahashi, K.; Cui, H.B.; Kobayashi, H.; Einaga, Y.; Sato, O. The light-induced excited spin state trapping effect on $Ni(dmit)_2$ salt with an Fe(III) spin-crossover cation: $[Fe(qsal)_2][Ni(dmit)_2].2CH_3CN$. *Chem. Lett.* **2005**, *34*, 1240–1241. [CrossRef]
45. Nihei, M.; Takahashi, N.; Nishikawa, H.; Oshio, H. Spin-crossover behavior and electrical conduction property in iron(II) complexes with tetrathiafulvalene moieties. *Dalton Trans.* **2011**, *40*, 2154–2156. [CrossRef] [PubMed]
46. Fukuroi, K.; Takahashi, K.; Mochida, T.; Sakurai, T.; Ohta, H.; Yamamoto, T.; Einaga, Y.; Mori, H. Synergistic spin transition between spin crossover and spin-peierls-like singlet formation in the halogen-bonded molecular hybrid system: $[Fe(iqsal)_2][Ni(dmit)_2]\cdot CH_3CN\cdot H_2O$. *Angew. Chem. Int. Ed. Engl.* **2014**, *53*, 1983–1986. [CrossRef] [PubMed]
47. Djukic, B.; Lemaire, M.T. Hybrid spin-crossover conductor exhibiting unusual variable-temperature electrical conductivity. *Inorg. Chem.* **2009**, *48*, 10489–10491. [CrossRef] [PubMed]
48. Faulmann, C.; Dorbes, S.; Real, J.A.; Valade, L. Electrical conductivity and spin crossover: Towards the first achievement with a metal bis dithiolene complex. *J. Low Temp. Phys.* **2006**, *142*, 261–266. [CrossRef]
49. Faulmann, C.; Jacob, K.; Dorbes, S.; Lampert, S.; Malfant, I.; Doublet, M.L.; Valade, L.; Real, J.A. Electrical conductivity and spin crossover: A new achievement with a metal bis dithiolene complex. *Inorg. Chem.* **2007**, *46*, 8548–8559. [CrossRef] [PubMed]
50. Takahashi, K.; Cui, H.B.; Okano, Y.; Kobayashi, H.; Einaga, Y.; Sato, O. Electrical conductivity modulation coupled to a high-spin-low-spin conversion in the molecular system $[FeIII(qsal)_2][Ni(dmit)_2]_3.CH_3CN.H_2O$. *Inorg. Chem.* **2006**, *45*, 5739–5741. [CrossRef] [PubMed]
51. Takahashi, K.; Cui, H.B.; Okano, Y.; Kobayashi, H.; Mori, H.; Tajima, H.; Einaga, Y.; Sato, O. Evidence of the chemical uniaxial strain effect on electrical conductivity in the spin-crossover conducting molecular system: $[FeIII(qnal)_2][Pd(dmit)_2]_5$.acetone. *J. Am. Chem. Soc.* **2008**, *130*, 6688–6689. [CrossRef] [PubMed]
52. Phan, H.; Benjamin, S.M.; Steven, E.; Brooks, J.S.; Shatruk, M. Photomagnetic response in highly conductive iron(ii) spin-crossover complexes with tcnq radicals. *Angew. Chem. Int. Ed. Engl.* **2015**, *54*, 823–827. [CrossRef] [PubMed]
53. Koo, Y.-S.; Galán-Mascarós, J.R. Spin crossover probes confer multistability to organic conducting polymers. *Adv. Mater.* **2014**, *26*, 6785–6789. [CrossRef] [PubMed]

54. Chen, Y.-C.; Meng, Y.; Ni, Z.-P.; Tong, M.-L. Synergistic electrical bistability in a conductive spin crossover heterostructure. *J. Mater. Chem. C* **2015**, *3*, 945–949. [CrossRef]
55. Gural'skiy, I.Y.A.; Quintero, C.M.; Costa, J.S.; Demont, P.; Molnar, G.; Salmon, L.; Shepherd, H.J.; Bousseksou, A. Spin crossover composite materials for electrothermomechanical actuators. *J. Mater. Chem. C* **2014**, *2*, 2949–2955. [CrossRef]
56. Matsuda, M.; Isozaki, H.; Tajima, H. Reproducible on-off switching of the light emission from the electroluminescent device containing a spin crossover complex. *Thin Solid Films* **2008**, *517*, 1465–1467. [CrossRef]
57. Mahfoud, T.; Molnar, G.; Cobo, S.; Salmon, L.; Thibault, C.; Vieu, C.; Demont, P.; Bousseksou, A. Electrical properties and non-volatile memory effect of the $[Fe(HB(pz)_3)_2]$ spin crossover complex integrated in a microelectrode device. *Appl. Phys. Lett.* **2011**, *99*, 053307. [CrossRef]
58. Shi, S.; Schmerber, G.; Arabski, J.; Beaufrand, J.B.; Kim, D.J.; Boukari, S.; Bowen, M.; Kemp, N.T.; Viart, N.; Rogez, G.; *et al*. Study of molecular spin-crossover complex $Fe(phen)_2(NCS)_2$ thin films. *Appl. Phys. Lett.* **2009**, *95*, 043303. [CrossRef]
59. Zhang, X.; Palamarciuc, T.; Letard, J.-F.; Rosa, P.; Lozada, E.V.; Torres, F.; Rosa, L.G.; Doudin, B.; Dowben, P.A. The spin state of a molecular adsorbate driven by the ferroelectric substrate polarization. *Chem. Commun.* **2014**, *50*, 2255–2257. [CrossRef] [PubMed]
60. Rotaru, A.; Dugay, J.; Tan, R.P.; Gural'skiy, I.A.; Salmon, L.; Demont, P.; Carrey, J.; Molnar, G.; Respaud, M.; Bousseksou, A. Nano-electromanipulation of spin crossover nanorods: Towards switchable nanoelectronic devices. *Adv. Mater.* **2013**, *25*, 1745–1749. [CrossRef] [PubMed]
61. Dugay, J.; Giménez-Marqués, M.; Kozlova, T.; Zandbergen, H.W.; Coronado, E.; van der Zant, H.S.J. Spin switching in electronic devices based on 2d assemblies of spin-crossover nanoparticles. *Adv. Mater.* **2015**, *27*, 1288–1293. [CrossRef] [PubMed]
62. Lefter, C.; Tan, R.; Tricard, S.; Dugay, J.; Molnár, G.; Salmon, L.; Carrey, J.; Rotaru, A.; Bousseksou, A. On the stability of spin crossover materials: From bulk samples to electronic devices. *Polyhedron* **2015**, *102*, 434–440. [CrossRef]
63. Lefter, C.; Tan, R.; Dugay, J.; Tricard, S.; Molnar, G.; Salmon, L.; Carrey, J.; Rotaru, A.; Bousseksou, A. Light induced modulation of charge transport phenomena across the bistability region in [fe(htrz)2(trz)](bf4) spin crossover micro-rods. *Phys. Chem. Chem. Phys.* **2015**, *17*, 5151–5154. [CrossRef] [PubMed]
64. Lefter, C.; Tan, R.; Dugay, J.; Tricard, S.; Molnar, G.; Salmon, L.; Carrey, J.; Nicolazzi, W.; Rotaru, A.; Bousseksou, A. Unidirectional electric field-induced spin-state switching in spin crossover based microelectronic devices. *Chem. Phys. Lett.* **2016**, *644*, 138–141. [CrossRef]
65. Etrillard, C.; Faramarzi, V.; Dayen, J.-F.; Letard, J.-F.; Doudin, B. Photoconduction in $[Fe(Htrz)_2(trz)](BF_4)\cdot H_2O$ nanocrystals. *Chem. Commun.* **2011**, *47*, 9663–9665. [CrossRef] [PubMed]
66. Prins, F.; Monrabal-Capilla, M.; Osorio, E.A.; Coronado, E.; van der Zant, H.S.J. Room-temperature electrical addressing of a bistable spin-crossover molecular system. *Adv. Mater.* **2011**, *23*, 1545–1549. [CrossRef] [PubMed]
67. Alam, M.S.; Stocker, M.; Gieb, K.; Muller, P.; Haryono, M.; Student, K.; Grohmann, A. Spin-state patterns in surface-grafted beads of iron(II) complexes. *Angew. Chem. Int. Ed. Engl.* **2010**, *49*, 1159–1163. [CrossRef] [PubMed]
68. Grohmann, A.; Haryono, M.; Student, K.; Müller, P.; Stocker, M. Mapping the spin state in spin-crossover complex assemblies: Current-imaging tunnelling spectroscopy (cits). *Eur. J. Inorg. Chem.* **2013**, *2013*, 662–669. [CrossRef]
69. Palamarciuc, T.; Oberg, J.C.; El Hallak, F.; Hirjibehedin, C.F.; Serri, M.; Heutz, S.; Letard, J.-F.; Rosa, P. Spin crossover materials evaporated under clean high vacuum and ultra-high vacuum conditions: From thin films to single molecules. *J. Mater. Chem.* **2012**, *22*, 9690–9695. [CrossRef]
70. Pronschinske, A.; Chen, Y.; Lewis, G.F.; Shultz, D.A.; Calzolari, A.; Buongiorno Nardelli, M.; Dougherty, D.B. Modification of molecular spin crossover in ultrathin films. *Nano Lett.* **2013**, *13*, 1429–1434. [CrossRef] [PubMed]
71. Gopakumar, T.G.; Matino, F.; Naggert, H.; Bannwarth, A.; Tuczek, F.; Berndt, R. Electron-induced spin crossover of single molecules in a bilayer on gold. *Angew. Chem. Int. Ed. Engl.* **2012**, *51*, 6262–6266. [CrossRef] [PubMed]

72. Miyamachi, T.; Gruber, M.; Davesne, V.; Bowen, M.; Boukari, S.; Joly, L.; Scheurer, F.; Rogez, G.; Yamada, T.K.; Ohresser, P.; *et al*. Robust spin crossover and memristance across a single molecule. *Nat. Commun.* **2012**, *3*, 938. [CrossRef] [PubMed]
73. Gruber, M.; Davesne, V.; Bowen, M.; Boukari, S.; Beaurepaire, E.; Wulfhekel, W.; Miyamachi, T. Spin state of spin-crossover complexes: From single molecules to ultrathin films. *Phys. Rev. B* **2014**, *89*, 195415. [CrossRef]
74. Gueddida, S.; Alouani, M. Spin crossover in a single $Fe(phen)_2(NCS)_2$ molecule adsorbed onto metallic substrates: An *ab initio* calculation. *Phys. Rev. B* **2013**, *87*, 144413. [CrossRef]
75. Osorio, E.A.; Moth-Poulsen, K.; van der Zant, H.S.J.; Paaske, J.; Hedegård, P.; Flensberg, K.; Bendix, J.; Bjørnholm, T. Electrical manipulation of spin states in a single electrostatically gated transition-metal complex. *Nano Lett.* **2009**, *10*, 105–110. [CrossRef] [PubMed]
76. Meded, V.; Bagrets, A.; Fink, K.; Chandrasekar, R.; Ruben, M.; Evers, F.; Bernand-Mantel, A.; Seldenthuis, J.S.; Beukman, A.; van der Zant, H.S.J. Electrical control over the Fe(II) spin crossover in a single molecule: Theory and experiment. *Phys. Rev. B* **2011**, *83*, 245415. [CrossRef]
77. Devid, E.J.; Martinho, P.N.; Kamalakar, M.V.; Šalitroš, I.; Prendergast, Ú.; Dayen, J.-F.; Meded, V.; Lemma, T.; González-Prieto, R.; Evers, F.; *et al*. Spin transition in arrays of gold nanoparticles and spin crossover molecules. *ACS Nano* **2015**, *9*, 4496–4507. [CrossRef] [PubMed]
78. Harzmann, G.D.; Frisenda, R.; van der Zant, H.S.J.; Mayor, M. Single-molecule spin switch based on voltage-triggered distortion of the coordination sphere. *Angew. Chem. Int. Ed. Engl.* **2015**, *54*, 13425–13430. [CrossRef] [PubMed]
79. Baadji, N.; Sanvito, S. Giant resistance change across the phase transition in spin-crossover molecules. *Phys. Rev. Lett.* **2012**, *108*, 217201. [CrossRef] [PubMed]
80. Aravena, D.; Ruiz, E. Coherent transport through spin-crossover single molecules. *J. Am. Chem. Soc.* **2012**, *134*, 777–779. [CrossRef] [PubMed]

© 2016 by the authors; licensee MDPI, Basel, Switzerland. This article is an open access article distributed under the terms and conditions of the Creative Commons by Attribution (CC-BY) license (http://creativecommons.org/licenses/by/4.0/).